Isomer Decay Spectroscopy of ^{164}Sm and ^{166}Gd: Midshell Collectivity Around $N = 100$

Z. Patel,[1,2] P.-A. Söderström,[2] Zs. Podolyák,[1] P. H. Regan,[1,3] P. M. Walker,[1] H. Watanabe,[2,4,5] E. Ideguchi,[6,7] G. S. Simpson,[8] H. L. Liu,[9] S. Nishimura,[2] Q. Wu,[10] F. R. Xu,[10] F. Browne,[2,11] P. Doornenbal,[2] G. Lorusso,[2] S. Rice,[1,2] L. Sinclair,[2,12] T. Sumikama,[13] J. Wu,[2,10] Z. Y. Xu,[14] N. Aoi,[6,7] H. Baba,[2] F. L. Bello Garrote,[15] G. Benzoni,[16] R. Daido,[7] Y. Fang,[7] N. Fukuda,[2] G. Gey,[8] S. Go,[17] A. Gottardo,[18] N. Inabe,[2] T. Isobe,[2] D. Kameda,[2] K. Kobayashi,[19] M. Kobayashi,[17] T. Komatsubara,[20,21] I. Kojouharov,[22] T. Kubo,[2] N. Kurz,[22] I. Kuti,[23] Z. Li,[24] M. Matsushita,[17] S. Michimasa,[17] C.-B. Moon,[25] H. Nishibata,[7] I. Nishizuka,[13] A. Odahara,[7] E. Şahin,[15] H. Sakurai,[2,14] H. Schaffner,[22] H. Suzuki,[2] H. Takeda,[2] M. Tanaka,[7] J. Taprogge,[26,27] Zs. Vajta,[23] A. Yagi,[7] and R. Yokoyama[28]

[1]*Department of Physics, University of Surrey, Guildford GU2 7XH, United Kingdom*
[2]*RIKEN Nishina Center, 2-1 Hirosawa, Wako-shi, Saitama 351-0198, Japan*
[3]*National Physical Laboratory, Teddington, Middlesex TW11 0LW, United Kingdom*
[4]*International Research Center for Nuclei and Particles in the Cosmos, Beihang University, Beijing 100191, China*
[5]*School of Physics and Nuclear Energy Engineering, Beihang University, Beijing 100191, China*
[6]*Research Center for Nuclear Physics (RCNP), Osaka University, Ibaraki, Osaka 567-0047, Japan*
[7]*Department of Physics, Osaka University, Machikaneyama-machi 1-1, Osaka 560-0043 Toyonaka, Japan*
[8]*LPSC, Université Joseph Fourier Grenoble 1, CNRS/IN2P3, Institut National Polytechnique de Grenoble, F-38026 Grenoble Cedex, France*
[9]*Department of Applied Physics, School of Science, Xi'an Jiaotong University, Xi'an 710049, China*
[10]*School of Physics and State Key Laboratory of Nuclear Physics and Technology, Peking University, Beijing 100871, China*
[11]*School of Computing, Engineering and Mathematics, University of Brighton, Brighton, BN2 4JG, United Kingdom*
[12]*Department of Physics, University of York, Heslington, York YO10 5DD, United Kingdom*
[13]*Department of Physics, Tohoku University, Aoba, Sendai, Miyagi 980-8578, Japan*
[14]*Department of Physics, University of Tokyo, Hongo, Bunkyo-ku, Tokyo 113-0033, Japan*
[15]*Department of Physics, University of Oslo, Oslo, Norway*
[16]*INFN Sezione di Milano, I-20133 Milano, Italy*
[17]*Center for Nuclear Study (CNS), University of Tokyo, Wako, Saitama 351-0198, Japan*
[18]*Instituto Nazionale di Fisica Nucleare, Laboratori Nazionali di Legnaro I-35020 Legnaro, Italy*
[19]*Department of Physics, Rikkyo University, 3-34-1 Nishi-Ikebukuro, Toshima-ku, Tokyo 171-8501, Japan*
[20]*Research Facility Center for Pure and Applied Science, University of Tsukuba, Ibaraki 305-8577, Japan*
[21]*Rare Isotope Science Project, Institute for Basic Science, Daejeon 305-811, Korea*
[22]*GSI Helmholtzzentrum für Schwerionenforschung GmbH, 64291 Darmstadt, Germany*
[23]*Institute for Nuclear Research, Hungarian Academy of Sciences, P. O. Box 51, Debrecen H-4001, Hungary*
[24]*School of Physics, Peking University, Beijing 100871, China*
[25]*Hoseo University, Asan, Chungnam 336-795, Korea*
[26]*Instituto de Estructura de la Materia, CSIC, E-28006 Madrid, Spain*
[27]*Departamento de Física Teórica, Universidad Autónoma de Madrid, E-28049 Madrid, Spain*
[28]*Center for Nuclear Study (CNS), University of Tokyo, Wako-shi, Saitama 351-0198, Japan*

(Received 27 August 2014; published 22 December 2014)

Excited states in the $N = 102$ isotones ^{166}Gd and ^{164}Sm have been observed following isomeric decay for the first time at RIBF, RIKEN. The half-lives of the isomeric states have been measured to be 950(60) and 600(140) ns for ^{166}Gd and ^{164}Sm, respectively. Based on the decay patterns and potential energy surface calculations, including β_6 deformation, a spin and parity of 6^- has been assigned to the isomeric states in both nuclei. Collective observables are discussed in light of the systematics of the region, giving insight into nuclear shape evolution. The decrease in the ground-band energies of ^{166}Gd and ^{164}Sm ($N = 102$) compared to ^{164}Gd and ^{162}Sm ($N = 100$), respectively, presents evidence for the predicted deformed shell closure at $N = 100$.

DOI: 10.1103/PhysRevLett.113.262502 PACS numbers: 23.20.Lv, 27.70.+q, 21.60.Ev, 23.35.+g

In the exploration of the nuclear landscape, it is evident that the neutron-rich side of stability contains a vast unknown territory, where approximately half of all the bound nuclides remain to be identified. Furthermore, this is the domain of rapid-neutron-capture (r process) nucleosynthesis, which is poorly understood and yet is key to the creation of chemical elements from iron to uranium ($Z = 26$–92) in stellar environments [1]. With the advent of the current generation of radioactive-beam facilities, it is now possible to address some of the open questions through experiment, and much effort has been devoted to the study of spherical neutron-rich closed-shell nuclides associated with the so-called "waiting points" of the r process. This is leading to an improved understanding of the elemental abundance peaks at $A \approx 80$ [2], $A \approx 130$ [3], and $A \approx 195$ [4].

In contrast, the present work is concerned with the enigmatic though less pronounced $A \approx 160$ abundance peak, believed to arise from strong midshell nuclear deformation, and to provide a unique probe of r-process conditions [5,6]. In this region, macroscopic-microscopic calculations [7] show a deformation maximum close to $N = 104$ and $Z = 66$ (^{170}Dy), which is simultaneously midshell for both neutrons and protons. However, these calculations seem to be contradicted by recent experimental data [8,9], which indicate either that the deformation maximum is at significantly lower proton and neutron numbers, or that there is more complex behavior, possibly due to energy gaps in the deformed single-particle space. In order to extend the experimental knowledge, and to test more recent theoretical calculations [10], we exploit a basic nuclear structure feature, namely, that deformation gives rise to long-lived nuclear excited states (isomers) [11]. Isomers with half-lives in the 100 ns to 100 μs range allow highly sensitive access to nuclear excited states following relativistic heavy-ion reactions [12]. Combined with the excellent uranium beam intensities from the Radioactive Ion Beam Factory (RIBF) facility at RIKEN, Japan [13], we have been able to reach further into the $A = 160$–170 midshell neutron-rich domain than was previously possible.

Neutron-rich $Z = 62, 64$ isotopes were produced by in-flight fission of a 345 A·MeV ^{238}U beam with an average beam intensity of 10 particle-nA incident on a ^{9}Be target at the RIBF. The nuclei of interest were separated and identified on an ion by ion basis using BigRIPS and the ZeroDegree spectrometers [13,14]. The nuclei were separated according to their mass-to-charge ratio (A/q) and atomic number (Z) by use of bending magnets for A/q separation and wedge degraders for energy loss (Z separation).

The ions of interest were implanted in a copper passive stopper, the use of which allows a high implantation rate. The γ rays emitted following isomeric decay were detected using EURICA (Euroball-RIKEN Cluster Array) [15–17]: 84 HPGe crystals arranged in a 4π configuration at $\sim$22 cm from implantation. The absolute efficiency of the array was 16.6% at 100 keV and 7.6% at 1 MeV. Ion implantation was correlated with the γ rays by use of an acquisition window of 100 μs which was opened when the ion passed through a plastic scintillator located $\sim$1 m upstream of implantation.

Delayed γ rays emitted from ^{166}Gd and ^{164}Sm are shown in Fig. 1. All labeled peaks have been identified and placed in the level schemes of ^{166}Gd and ^{164}Sm.

The level schemes seen in Fig. 2 and Fig. 3 were deduced from γ-γ coincidence analysis. The 70, 78, and 137 keV

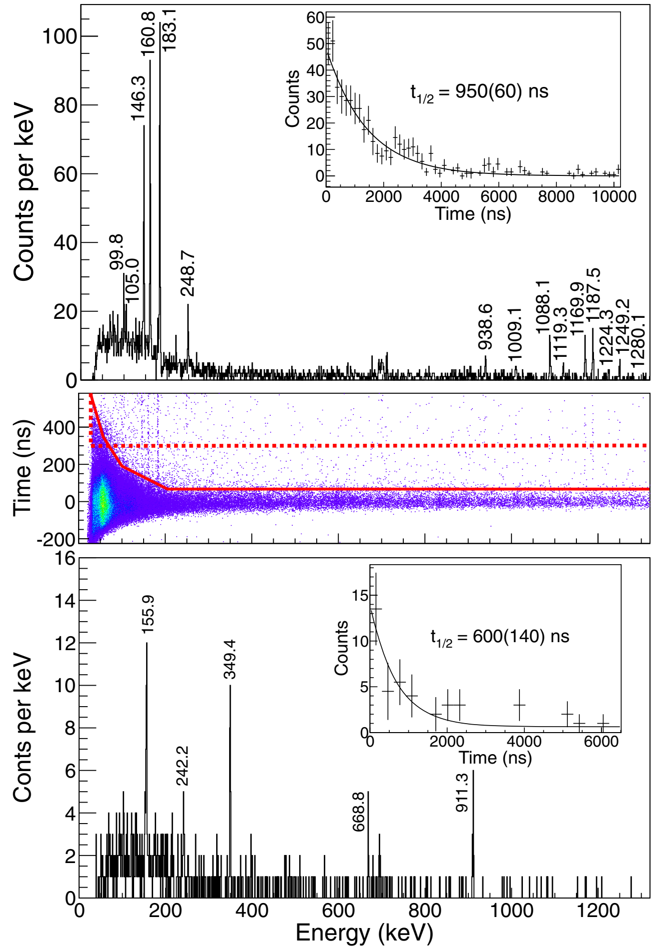

FIG. 1 (color online). Top: Spectrum of γ rays from ^{166}Gd, emitted within 2.5 μs after an ion's arrival. Middle: The prompt flash time cut (solid line) and the fixed time cut (dotted line) applied to the energy-time matrix. The former was used to produce the spectra shown above and the latter for determining γ-ray intensities. Bottom: Spectrum of γ rays from ^{164}Sm, emitted within 2 μs after an ion's arrival. Insets: The exponential decay curve from the isomeric decay of ^{166}Gd and ^{164}Sm.

γ rays in ^{166}Gd cannot be seen in Fig. 1, but have been observed in coincident γ-ray spectra. The existence of the 37 keV transition was deduced from the coincident relationship between the 146 and 1188 keV transitions. The $2^+ \to 0^+$ transition in ^{164}Sm was not observed, due to the relatively low efficiency for γ-ray detection in the 70 keV region, together with large $E2$ conversion coefficients for such transitions. The intensities of the transitions are listed in Table I and Table II. We note that a previous experiment tentatively assigned the $2^+ \to 0^+$ and $4^+ \to 2^+$ transitions in ^{166}Gd to 69.7 and 160.8 keV, respectively [18].

In addition to the γ rays assigned to ^{166}Gd, two weak γ rays of 220 and 269 keV were observed but not placed in the level scheme. The possibility that the identified γ rays are due to lower mass isotopes with one, two, or three

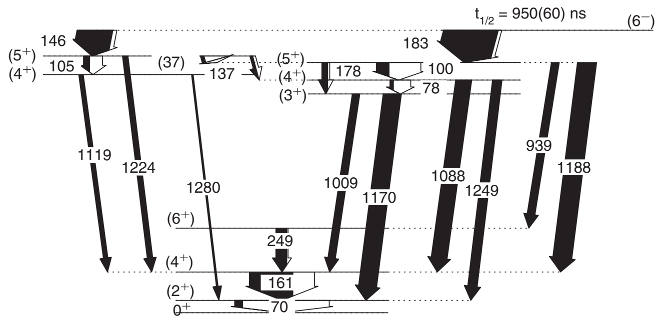

FIG. 2. Level scheme of ^{166}Gd obtained in this work.

electrons (H-like, He-like, and Li-like, respectively) was ruled out by comparing the data with known γ transitions in these isotopes. A γ-ray transition of energy 694 keV is also observed in ^{164}Sm. However, due to low statistics this could not be placed in the level scheme.

The spin and parity assignments given in Fig. 2 and Fig. 3 are based on the transition multipolarities obtained from the intensity balances through the levels and the decay patterns. For example, the strong 146 and 183 keV transitions, depopulating the isomeric state in ^{166}Gd, are assigned as $E1$ transitions. These assignments are necessitated by the low electron conversion coefficients required by the intensity balances. In the absence of directly measured electron conversion coefficients or γ-ray angular correlations, we consider our spin and parity assignments to be tentative.

The half-lives of the isomeric states were found from the exponential decay curves (see inset in Fig. 1) derived from the time between ion implantation and γ-ray detection. Energy gates were placed around the strong 146, 161, 183, 249, 1088, 1170, and 1188 keV γ rays in ^{166}Gd and the 155, 242, 349, 669, and 911 keV γ rays in ^{164}Sm, with background subtraction to improve accuracy. The half-lives of ^{166}Gd and ^{164}Sm were measured to have weighted averages of 950(60) and 600(140) ns, respectively. The half-lives were determined for all individual transitions of ^{166}Gd and ^{164}Sm, and were found to be consistent with each other within statistical uncertainties (in each nucleus), which suggests that all transitions in each nucleus are from the decay of a single isomeric state.

Potential energy surface calculations were made in order to further understand the nature of the level schemes of these isotones. The calculations included configuration constraints where the total energy was minimized in the (β_2, β_4, β_6) deformation space. For more details see Refs. [19,20]. The results can be seen in Table III. We note that significantly nonzero β_6 values are found, which alter the relative two-quasiparticle energies by up to 250 keV (compared to $\beta_6 = 0$ calculations). Indeed, the tables of Moller *et al.* [7] indicate that β_6 maximizes for ^{164}Sm and its inclusion in the calculation of multiquasiparticle states is necessary. These calculations suggest that a 6^- state with a two-neutron $\nu\frac{5}{2}^-[512] \otimes \nu\frac{7}{2}^+[633]$

TABLE I. Initial level energy E_i, spin parity J^π_i, and branching ratio B_tot (corrected for electron conversion) of the levels obtained for ^{166}Gd in this work. For each γ ray the energy E_γ, γ-ray intensity I_γ relative to the 183 keV γ-ray intensity, and final level spin J^π_f are listed. Transitions marked with * are only visible in coincident spectra, while ** indicates that the transition has not been directly observed but deduced from coincident relationships. Intensities marked † have not been directly measured but are obtained from the intensity balance of incoming and outgoing γ rays.

E_i (keV)	J^π_i	E_γ (keV)	I_γ(rel.)	B_tot(rel.)	J^π_f
70	(2^+)	$70(1)^*$	$15(1)^\dagger$	$100^\dagger$	0^+
230.8	(4^+)	160.8(2)	82(6)	100	(2^+)
479.5	(6^+)	248.7(3)	21(3)	100	(4^+)
1239.9	(3^+)	1009.1(7)	14(4)	29(10)	(4^+)
		1169.9(3)	34(7)	71(18)	(2^+)
1318.9	(4^+)	$78(1)^*$	$7(2)^\dagger$	$41(12)^\dagger$	(3^+)
		1088.1(3)	30(6)	37(9)	(4^+)
		1249.2(3)	18(5)	22(7)	(2^+)
1350.1	(4^+)	1119.3(3)	8(3)	74(36)	(4^+)
		1280.1(2)	3(1)	26(14)	(2^+)
1418.3	(5^+)	99.8(3)	24(3)	52(9)	(4^+)
		178.3(2)	11(2)	11(2)	(3^+)
		938.6(4)	15(4)	11(3)	(6^+)
		1187.5(3)	36(7)	26(6)	(4^+)
1455.1	(5^+)	37^{**}	$7(4)^\dagger$	$38(21)^\dagger$	(5^+)
		$137(1)^*$	$5(3)^\dagger$	$11(7)^\dagger$	(4^+)
		105.0(3)	12(2)	38(13)	(4^+)
		1224.3(3)	10(4)	12(6)	(4^+)
1601.4	(6^-)	146.3(2)	66(5)	41(4)	(5^+)
		183.1(2)	100	59(5)	(5^+)

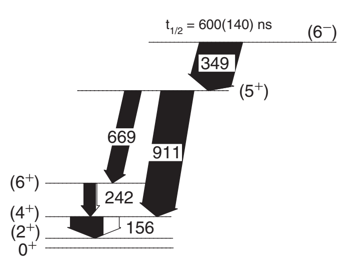

FIG. 3. Level scheme of ^{164}Sm obtained in this work.

TABLE II. Same as Table I, but for ^{164}Sm. Level energies are given relative to the first 2^+ state and γ-ray intensities I_γ are relative to the 349 keV γ-ray intensity.

$E_i - E(2^+)$ (keV)	J^π_i	E_γ (keV)	B_tot(rel.)	I_γ(rel.)	J^π_f
155.9(4)	(4^+)	155.9(4)	100	79(14)	(2^+)
398.1(5)	(6^+)	242.2(3)	100	28(9)	(4^+)
1067.2(5)	(5^+)	668.8(4)	66(28)	39(14)	(6^+)
		911.3(3)	100(40)	79(22)	(4^+)
1416.6(5)	(6^-)	349.4(2)	100	100	(5^+)

TABLE III. Low-lying quasiparticle states in ^{166}Gd and ^{164}Sm, predicted by potential energy surface calculations. Those marked with * are energetically unfavored configurations according to the residual spin-spin coupling rule; therefore, an average 200 keV energy has been added to these states. The calculations give $\gamma = 0$ for all predicted states.

K^π	Configuration	β_2	β_4	β_6	E_x (MeV)
^{166}Gd					
g.s.		0.296	0.015	−0.020	
6^-	$\nu\frac{5}{2}^-[512] \otimes \nu\frac{7}{2}^+[633]$	0.291	0.014	−0.017	1.288*
4^+	$\pi\frac{3}{2}^+[411] \otimes \pi\frac{5}{2}^+[413]$	0.299	0.017	−0.022	1.300
3^+	$\nu\frac{1}{2}^-[521] \otimes \nu\frac{5}{2}^-[512]$	0.292	0.015	−0.018	1.400
4^-	$\nu\frac{1}{2}^-[521] \otimes \nu\frac{7}{2}^+[633]$	0.284	0.015	−0.013	1.684
4^-	$\pi\frac{3}{2}^+[411] \otimes \pi\frac{5}{2}^-[532]$	0.287	0.011	−0.015	1.769*
5^-	$\pi\frac{5}{2}^+[413] \otimes \pi\frac{5}{2}^-[532]$	0.289	0.013	−0.017	1.826
^{164}Sm					
g.s.		0.301	0.030	−0.023	
6^-	$\nu\frac{5}{2}^-[512] \otimes \nu\frac{7}{2}^+[633]$	0.295	0.029	−0.020	1.301*
5^-	$\pi\frac{5}{2}^+[413] \otimes \pi\frac{5}{2}^-[532]$	0.294	0.027	−0.020	1.411
4^-	$\pi\frac{3}{2}^+[411] \otimes \pi\frac{5}{2}^-[532]$	0.295	0.027	−0.021	1.907*
4^-	$\pi\frac{5}{2}^+[413] \otimes \pi\frac{3}{2}^-[541]$	0.285	0.018	−0.020	2.195
4^+	$\pi\frac{5}{2}^-[532] \otimes \pi\frac{3}{2}^-[541]$	0.280	0.015	−0.016	2.502*

configuration is isomeric in both ^{164}Sm and ^{166}Gd. Analogous 6^- states have previously been observed in heavier $N = 102$ isotones ^{170}Er ($Z = 68$) at 1591 keV [21] and in ^{172}Yb ($Z = 70$) at 1550 keV [22]. The isomeric states in both ^{164}Sm and ^{166}Gd are assigned (6^-) spin and parity.

A fragment of a two-quasiparticle band has been observed in ^{166}Gd with a possible (4^+) bandhead at 1350 keV. Calculations suggest a two-proton $\pi\frac{3}{2}^+[411] \otimes \pi\frac{5}{2}^+[413]$ configuration (see Table III). Such bands have been observed in isotopes ^{156}Gd [23] and ^{160}Gd [24] at 1511 and 1070 keV, respectively, which is consistent with our configuration assignment.

The third band observed in ^{166}Gd is assigned as the vibrational γ band. The bandhead was not observed; however, the energies and spacings of the assigned (3^+), (4^+), and (5^+) levels (1240, 1318, and 1418 keV, respectively) are similar to those in the isotones ^{172}Yb (1173, 1263, and 1376 keV, respectively) [22] and ^{170}Er (1010, 1127, and (1237) keV, respectively) [21]. Based on the isotones' 2^+ bandheads (1118 keV for ^{172}Yb and 934 keV for ^{170}Er) and the (3^+), (4^+), and (5^+) levels of ^{166}Gd, the 2^+ bandhead for ^{166}Gd is estimated to be at ≈1190 keV. The (5^+) level in ^{164}Sm likely belongs to its corresponding γ band. However, the lack of statistics does not allow further determination of the γ-band members. The assignment of (5^+) spin and parity to this level is consistent with the $E1$ multipolarity assignment of the 349 keV transition depopulating the (6^-) isomeric state.

Different quasiparticle configurations may have different spin projections K on the symmetry axis of the deformed nucleus. Transitions between states with different K values can be forbidden by the $\Delta K \leq \lambda$ selection rule, where λ is the multipole order of the transition. K forbiddenness can result in long-lived states at high excitation energy [11] like the ones observed in this work. The hindrance factor is strongly correlated with the degree of forbiddenness, $\nu = \Delta K - \lambda$. The reduced hindrance of a transition is then defined using the partial half-life relative to the single-particle Weisskopf estimate, expressed as $f_\nu = (T^\gamma_{1/2}/T^W_{1/2})^{1/\nu}$ [11]. The ^{166}Gd (6^-) isomer decays via a 183 keV $E1$ transition to the γ band ($\nu = 3$) with a reduced hindrance of $f_\nu = 356(7)$ and the ^{164}Sm (6^-) isomer decays to the γ band via a 349 keV $E1$ transition with $f_\nu = 487(38)$. These are similar values which are also broadly in agreement with the analysis of Löbner [25]. The (6^-) isomer in ^{166}Gd also decays via a 146 keV $E1$ transition to the $K = 4$ band ($\nu = 1$). The reduced hindrance is $f_\nu = 3.77(24) \times 10^7$, in accordance with the large change in valence nucleons required for this transition: the two-neutron quasiparticle state decays and a two-proton quasiparticle state is created.

A key feature of our results is that the isomers decay to low-lying excited states, which can themselves be used to deduce basic nuclear structure information. Especially useful are the first 2^+ and 4^+ energies. Systematics of $E(2^+)$ and $E(4^+ \rightarrow 2^+)$ are shown in Fig. 4. The observed 2^+ and 4^+ energies of ^{166}Gd and ^{164}Sm are the lowest in their isotopic chains and of the $N = 102$ isotones. This suggests that these are the most deformed $N = 102$ nuclei observed in this region to date, although a further decrease in energy with decreasing Z can be expected for Nd ($Z = 60$). These new points in the systematics also highlight the increase of $E(2^+)$ and $E(4^+ \rightarrow 2^+)$ at $N = 100$. An increase in $E(2^+)$ and $E(4^+ \rightarrow 2^+)$ at $N = 100$ in the Dy chain was previously observed. However, it was unclear

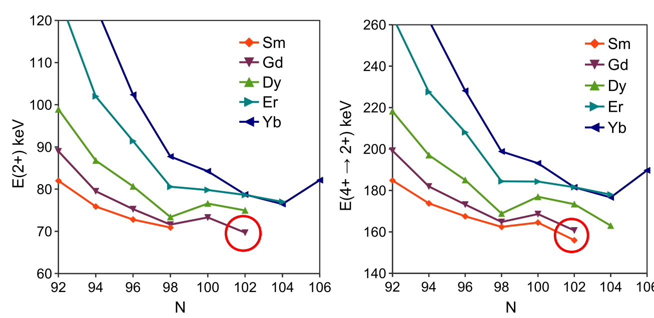

FIG. 4 (color online). Systematics of $E(2^+)$ and $E(4^+ \rightarrow 2^+)$ for Sm, Gd, Dy, Er, and Yb isotopes. All data points from [26] and this work.

if this increase is due to a local minimum at $N = 98$ or a local maximum at $N = 100$.

Our total energy surface calculations predict a smooth increase of β_2 deformation with increasing neutron number. Maximum deformation is reached at $N = 102$ with $\beta_2 =$ 0.296 and 0.301, respectively, for Gd and Sm isotopes. Other calculations show a similar picture. For example, Moller *et al.* [7] also predict a smooth change in β_2 deformation, with a maximum at $N = 102$ for Sm ($Z = 62$), Gd ($Z = 64$), and Dy ($Z = 66$).

There have been several calculations performed on Dy isotopes due to its midshell Z value. Hartree-Fock calculations using a variety of Skyrme parametrizations were performed on Dy isotopes in Ref. [27]. The majority of Skyrme forces predict a maximum deformation at $N = 102$, while others place it at $N = 100$. Total energy surface calculations of the type used in the present Letter were performed in Ref. [28] for Dy, showing greater deformation at $N = 102$ compared to $N = 104$ and $N = 106$, while those of Ref. [29] place the maximum at $N = 100$ using a cranked mean-field approach. More recently, a microscopic study based on the pseudo-SU(3) model also predicts a maximum deformation at $N = 102$ [30].

These calculations are all consistent in predicting a smooth β_2 deformation change in Sm, Gd, and Dy isotopic chains. In contrast, the energy systematics of Sm, Gd, and Dy isotopes do not change smoothly with N (see Fig. 4). The $E(2^+)$ is larger at $N = 100$ than at $N = 98$ and $N = 102$. The systematics of Dy suggest that the $E(2^+)$ at $N = 98$ is unexpectedly low. The same is valid, although to a lesser extent, in the heavier Er and Yb isotopes. However, in Gd and Sm isotopes the $E(2^+)$ and $E(4^+ \rightarrow 2^+)$ values at $N = 100$ appear higher than the systematic trends suggest. Analysis of $E(2^+)$, $E(4^+ \rightarrow 2^+)$ (see Fig. 4) and $E(6^+ \rightarrow 4^+)$ all suggest the same picture: unexpectedly low energies at $N = 98$ for Dy, Er, and Yb, and unexpectedly high energies at $N = 100$ for Gd and Sm.

Remarkably, the most recent projected Hartree-Fock calculations performed by Ghorui *et al.* for neutron-rich Sm isotopes [10], and now also for Gd isotopes [31], in fact show a slightly increased $E(2^+)$ energy at $N = 100$ compared to $N = 98$ and $N = 102$ (Sm only). Their emphasis was on the prediction of a deformed shell gap at $N = 100$, along with a smooth change in β_2 deformation throughout the isotopic chains. Other calculations using relativistic mean-field formalism had already suggested $N = 100$ to be a deformed magic number [32,33]. These calculations also show that a deformed shell closure would have an effect on the masses of $Z \leq 62$ nuclei (^{164}Sm, ^{162}Nd, ^{160}Ce, and ^{158}Ba) which manifests as a discontinuity of the two-neutron separation energies. However, these nuclei are far from stability and, according to the recent AME2012 atomic mass evaluation, the masses of these nuclei are unknown [34]. Where such information exists ($Z \geq 70$) there is no evidence for the deformed magicity of $N = 100$. However, the anomalous $E(2^+)$ behavior has been observed in Dy isotopes [9], and more prominently here in Gd and Sm isotopes, clearly highlighting complex deformation variations. This behavior gives support to the appearance of a deformed $N = 100$ shell gap for $Z \leq 66$, and this will influence r-process abundance calculations [5,6]. Confirmation through mass measurements is now needed in order to clarify the remarkable structure evolution in this doubly midshell region. Further investigation of the role of β_6 deformation is also warranted.

In summary, excited states in ^{166}Gd and ^{164}Sm have been observed from the decay of newly found isomeric states with half-lives of 950(60) and 600(140) ns, respectively. Total energy surface calculations are in agreement with a 6^- spin-parity assignment for these isomers, with a $\nu\frac{5}{2}^-[512] \otimes \nu\frac{7}{2}^+[633]$ configuration. A local maximum of the ground-band energies at $N = 100$ is revealed for Sm and Gd isotopes.

This work was carried out at the RIBF operated by RIKEN Nishina Center, RIKEN and CNS, University of Tokyo. All UK authors are supported by STFC. P. H. R. is partially supported by the UK National Measurement Office (NMO). P.-A. S. was financed by JSPS Grant No. 23.01752 and the RIKEN Foreign Postdoctoral Researcher Program. J. T. was financed by Spanish Ministerio de Ciencia e Innovación under Contracts No. FPA2009-13377-C02 and No. FPA2011-29854-C04. Zs. V. and I. K. were supported by OTKA Contract No. K100835. We acknowledge the EUROBALL Owners Committee for the loan of germanium detectors and the PreSpec Collaboration for the readout electronics of the cluster detectors. This work was supported by JSPS KAKENHI Grant No. 25247045.

[1] E. M. Burbidge, G. R. Burbidge, W. A. Fowler, and F. Hoyle, Rev. Mod. Phys. **29**, 547 (1957).

[2] J. A. Winger, S. V. Ilyushkin, K. P. Rykaczewski, C. J. Gross, J. C. Batchelder, C. Goodin, R. Grzywacz, J. H. Hamilton, A. Korgul, W. Królas *et al.*, Phys. Rev. Lett. **102**, 142502 (2009).

[3] A. Jungclaus, L. Cáceres, M. Górska, M. Pfützner, S. Pietri, E. Werner-Malento, H. Grawe, K. Langanke, G. Martínez-Pinedo, F. Nowacki *et al.*, Phys. Rev. Lett. **99**, 132501 (2007).

[4] A. I. Morales, J. Benlliure, T. Kurtukián-Nieto, K.-H. Schmidt, S. Verma, P. H. Regan, Z. Podolyák, M. Górska, S. Pietri, R. Kumar *et al.*, Phys. Rev. Lett. **113**, 022702 (2014).

[5] R. Surman, J. Engel, J. R. Bennett, and B. S. Meyer, Phys. Rev. Lett. **79**, 1809 (1997).

[6] M. R. Mumpower, G. C. McLaughlin, and R. Surman, Phys. Rev. C **85**, 045801 (2012).

[7] P. Moller, J. Nix, W. Myers, and W. Swiatecki, At. Data Nucl. Data Tables **59**, 185 (1995).

[8] E. F. Jones, J. H. Hamilton, P. M. Gore, A. V. Ramayya, J. K. Hwang, A. P. deLima, S. J. Zhu, Y. X. Luo, C. J. Beyer, J. Kormicki *et al.*, J. Phys. G **30**, L43 (2004).
[9] P.-A. Söderström, J. Nyberg, P. H. Regan, A. Algora, G. de Angelis, S. F. Ashley, S. Aydin, D. Bazzacco, R. J. Casperson, W. N. Catford *et al.*, Phys. Rev. C **81**, 034310 (2010).
[10] S. K. Ghorui, B. B. Sahu, C. R. Praharaj, and S. K. Patra, Phys. Rev. C **85**, 064327 (2012).
[11] P. Walker and G. Dracoulis, Nature (London) **399**, 35 (1999).
[12] S. J. Steer, Z. Podolyák, S. Pietri, M. Górska, H. Grawe, K. H. Maier, P. H. Regan, D. Rudolph, A. B. Garnsworthy, R. Hoischen *et al.*, Phys. Rev. C **84**, 044313 (2011).
[13] Y. Yano, Nucl. Instrum. Methods Phys. Res., Sect. B **261**, 1009 (2007).
[14] T. Kubo, D. Kameda, H. Suzuki, N. Fukuda, H. Takeda, Y. Yanagisawa, M. Ohtake, K. Kusaka, K. Yoshida, N. Inabe *et al.*, Prog. Theor. Exp. Phys. **2012**, 03C003.
[15] S. Nishimura, Prog. Theor. Exp. Phys. **2012**, 03C006 (2012).
[16] S. Nishimura, Nucl. Phys. News Int. **22**, 38 (2012).
[17] P.-A. Söderström, S. Nishimura, P. Doornenbal, G. Lorusso, T. Sumikama, H. Watanabe, Z. Xu, H. Baba, F. Browne, S. Go *et al.*, Nucl. Instrum. Methods Phys. Res., Sect. B **317**, 649 (2013).
[18] A. Osa, S. Ichikawa, M. Matsuda, T. K. Sato, and S.-C. Jeong, Nucl. Instrum. Methods Phys. Res., Sect. B **266**, 4394 (2008).
[19] F. Xu, P. Walker, J. Sheikh, and R. Wyss, Phys. Lett. B **435**, 257 (1998).
[20] H. L. Liu, F. R. Xu, P. M. Walker, and C. A. Bertulani, Phys. Rev. C **83**, 011303 (2011).
[21] G. D. Dracoulis, G. J. Lane, F. G. Kondev, H. Watanabe, D. Seweryniak, S. Zhu, M. P. Carpenter, C. J. Chiara, R. V. F. Janssens, T. Lauritsen *et al.*, Phys. Rev. C **81**, 054313 (2010).
[22] R. Nordhagen, R. Diamond, and F. Stephens, Nucl. Phys. **A138**, 231 (1969).
[23] H. Daley and M. Nagarajan, Phys. Lett. B **166**, 379 (1986).
[24] C. W. Reich, Nucl. Data Sheets **105**, 557 (2005).
[25] K. Löbner, Phys. Lett. B **26**, 369 (1968).
[26] Data extracted using the NNDC On-Line Data Service from the ENSDF database, file revised as of October 21, 2014.
[27] A. K. Rath, P. D. Stevenson, P. H. Regan, F. R. Xu, and P. M. Walker, Phys. Rev. C **68**, 044315 (2003).
[28] P. H. Regan, F. R. Xu, P. M. Walker, M. Oi, A. K. Rath, and P. D. Stevenson, Phys. Rev. C **65**, 037302 (2002).
[29] H. L. Yadav, M. Kaushik, I. R. Jakhar, and A. Ansari, Part. Nucl. Lett. **112** (2002).
[30] C. Vargas, V. Velázquez, and S. Lerma, The European Physical Journal A **49**, 4 (2013).
[31] S. Patra (private communication).
[32] L. Satpathy and S. Patra, Nucl. Phys. **A722**, C24 (2003).
[33] L. Satpathy and S. Patra, J. Phys. G **30**, 771 (2004).
[34] M. Wang, G. Audi, A. Wapstra, F. Kondev, M. MacCormick, X. Xu, and B. Pfeiffer, Chin. Phys. C **36**, 1603 (2012).